

Examination of the production of an isotensor dibaryon in the $pp \rightarrow pp\pi^+\pi^-$ reaction

P. Adlarson,¹ W. Augustyniak,² W. Bardan,³ M. Bashkanov,⁴ F. S. Bergmann,⁵ M. Berłowski,⁶ A. Bondar,^{7,8} M. Büscher,^{9,10} H. Calén,¹ I. Ciepał,¹¹ H. Clement,^{12,13,*} E. Czerwiński,³ K. Demmich,⁵ R. Engels,¹⁴ A. Erven,¹⁵ W. Erven,¹⁵ W. Eyrich,¹⁶ P. Fedorets,^{14,17} K. Föhl,¹⁸ K. Fransson,¹ F. Goldenbaum,¹⁴ A. Goswami,^{14,19} K. Grigoryev,^{14,20} L. Heijmanskjöld,^{1,†} V. Hejny,¹⁴ N. Hüskens,⁵ L. Jarczyk,³ T. Johansson,¹ B. Kamys,³ G. Kemmerling,^{15,‡} A. Khoukaz,⁵ O. Khreptak,³ D. A. Kirillov,²¹ S. Kistryn,³ H. Kleines,^{15,‡} B. Klos,²² W. Krzemień,⁶ P. Kulesa,¹¹ A. Kupść,^{1,6} K. Lalwani,²³ D. Lersch,^{14,§} B. Lorentz,¹⁴ A. Magiera,³ R. Maier,^{14,24} P. Marciniowski,¹ B. Mariański,² H.-P. Morsch,² P. Moskal,³ H. Ohm,¹⁴ W. Parol,¹¹ E. Perez del Rio,^{12,13,||} N. M. Piskunov,²¹ D. Prasuhn,¹⁴ D. Pszczel,^{1,6} K. Pysz,¹¹ J. Ritman,^{14,24,25} A. Roy,¹⁹ Z. Rudy,³ O. Rundel,³ S. Sawant,²⁶ S. Schadmand,¹⁴ I. Schätti-Ozerianska,³ T. Sefzick,¹⁴ V. Serdyuk,¹⁴ B. Shwartz,^{7,8} T. Skorodko,^{12,13,27} M. Skurzok,³ J. Smyrski,³ V. Sopov,¹⁷ R. Stassen,¹⁴ J. Stepaniak,⁶ E. Stephan,²² G. Sterzenbach,¹⁴ H. Stockhorst,¹⁴ H. Ströher,^{14,24} A. Szczurek,¹¹ A. Trzciński,² M. Wolke,¹ A. Wrońska,³ P. Wüstner,¹⁵ A. Yamamoto,²⁸ J. Zabierowski,²⁹ M. J. Zieliński,³ J. Złomańczuk,¹ P. Żuprański,² and M. Żurek¹⁴

(WASA-at-COSY Collaboration)

¹*Division of Nuclear Physics, Department of Physics and Astronomy, Uppsala University, Box 516, 75120 Uppsala, Sweden*

²*Nuclear Physics Division, National Centre for Nuclear Research, ul. Hoza 69, 00-681 Warsaw, Poland*

³*Institute of Physics, Jagiellonian University, prof. Stanisława Łojasiewicza 11, 30-348 Kraków, Poland*

⁴*Department of Physics, University of York, Heslington, York YO10 5DD, United Kingdom*

⁵*Institut für Kernphysik, Westfälische Wilhelms-Universität Münster, Wilhelm-Klemm-Str. 9, 48149 Münster, Germany*

⁶*High Energy Physics Division, National Centre for Nuclear Research, ul. Hoza 69, 00-681 Warsaw, Poland*

⁷*Budker Institute of Nuclear Physics of SB RAS, 11 Acad. Lavrentieva Pr., Novosibirsk, 630090 Russia*

⁸*Novosibirsk State University, 2 Pirogova Str., Novosibirsk, 630090 Russia*

⁹*Peter Grünberg Institut, PGI-6 Elektronische Eigenschaften, Forschungszentrum Jülich, 52425 Jülich, Germany*

¹⁰*Institut für Laser- und Plasmaphysik, Heinrich Heine Universität Düsseldorf, Universitätsstr. 1, 40225 Düsseldorf, Germany*

¹¹*The Henryk Niewodniczański Institute of Nuclear Physics, Polish Academy of Sciences, ul. Radzikowskiego 152, 31-342 Kraków, Poland*

¹²*Physikalisches Institut, Eberhard Karls Universität Tübingen, Auf der Morgenstelle 14, 72076 Tübingen, Germany*

¹³*Kepler Center for Astro and Particle Physics, Physikalisches Institut der Universität Tübingen, Auf der Morgenstelle 14, 72076 Tübingen, Germany*

¹⁴*Institut für Kernphysik, Forschungszentrum Jülich, 52425 Jülich, Germany*

¹⁵*Zentralinstitut für Engineering, Elektronik und Analytik, Forschungszentrum Jülich, 52425 Jülich, Germany*

¹⁶*Physikalisches Institut, Friedrich-Alexander Universität Erlangen-Nürnberg, Erwin-Rommel-Str. 1, 91058 Erlangen, Germany*

¹⁷*Institute for Theoretical and Experimental Physics named by A.I. Alikhanov of National Research Centre “Kurchatov Institute”, 25 Bolshaya Cheremushkinskaya Str., Moscow, 117218 Russia*

¹⁸*II. Physikalisches Institut, Justus-Liebig-Universität Gießen, Heinrich-Buff-Ring 16, 35392 Giessen, Germany*

¹⁹*Discipline of Physics, Indian Institute of Technology Indore, Khandwa Road, Indore, Madhya Pradesh 453 552, India*

²⁰*High Energy Physics Division, Petersburg Nuclear Physics Institute named by B.P. Konstantinov of National Research Centre “Kurchatov Institute”, 1 mkr. Orlova roshcha, Leningradskaya Oblast, Gatchina, 188300 Russia*

²¹*Veksler and Baldin Laboratory of High Energy Physics, Joint Institute for Nuclear Physics, 6 Joliot-Curie, Dubna, 141980 Russia*

²²*August Chelkowski Institute of Physics, University of Silesia, ul. 75 Pułku Piechoty 1, 41-500 Chorzów, Poland*

²³*Department of Physics, Malaviya National Institute of Technology Jaipur, JLN Marg, Jaipur, Rajasthan 302 017, India*

²⁴*JARA-FAME, Jülich Aachen Research Alliance, Forschungszentrum Jülich, 52425 Jülich, and RWTH Aachen, 52056 Aachen, Germany*

²⁵*Institut für Experimentalphysik I, Ruhr-Universität Bochum, Universitätsstr. 150, 44780 Bochum, Germany*

²⁶*Department of Physics, Indian Institute of Technology Bombay, Powai, Mumbai, Maharashtra 400 076, India*

²⁷*Department of Physics, Tomsk State University, 36 Lenin Ave., Tomsk, 634050 Russia*

²⁸*High Energy Accelerator Research Organisation KEK, Tsukuba, Ibaraki 305-0801, Japan*

²⁹*Astrophysics Division, National Centre for Nuclear Research, Box 447, 90-950 Łódź, Poland*



(Received 13 August 2018; published 4 February 2019)

*Corresponding author: heinz.clement@uni-tuebingen.de

[†]Present address: Institut für Kernphysik, Johannes Gutenberg Universität Mainz, Johann-Joachim-Becher Weg 45, 55128 Mainz, Germany.

[‡]Present address: Jülich Centre for Neutron Science JCNS, Forschungszentrum Jülich, 52425 Jülich, Germany.

[§]Present address: Department of Physics, Florida State University, 77 Chieftan Way, Tallahassee, FL 32306-4350, USA.

^{||}Present address: INFN, Laboratori Nazionali di Frascati, Via E. Fermi, 40, 00044 Frascati (Roma), Italy.

The quasifree $pp \rightarrow pp\pi^+\pi^-$ reaction has been measured by means of pd collisions at $T_p = 1.2$ GeV using the WASA detector setup at COSY enabling exclusive and kinematically complete measurements. Total and differential cross sections have been extracted for the energy region $T_p = 1.08$ – 1.36 GeV ($\sqrt{s} = 2.35$ – 2.46 GeV) covering thus the regions of $N^*(1440)$ and $\Delta(1232)\Delta(1232)$ resonance excitations. Calculations describing these excitations by t -channel meson exchange as well as isospin relations based on the $pp \rightarrow pp\pi^0\pi^0$ data underpredict substantially the measured total cross section. The calculations are also at variance with specific experimental differential cross sections. An isotensor ΔN dibaryon resonance with $I(J^P) = 2(1^+)$ produced associatedly with a pion is able to overcome these deficiencies. Such a dibaryon was predicted by Dyson and Xuong [Phys. Rev. Lett. **13**, 815 (1964)] and more recently calculated by A. Gal and H. Garcilazo [Nucl. Phys. A **928**, 73 (2014)].

DOI: 10.1103/PhysRevC.99.025201

I. INTRODUCTION

Early measurements of two-pion production initiated by nucleon-nucleon (NN) collisions were conducted with bubble chambers, where due to low statistics primarily only results for total cross sections were obtained [1–7]. In recent years the two-pion production has been measured from threshold up to incident energies of $T_p = 1.4$ GeV with high accuracy by exclusive and kinematically complete experiments conducted at CELSIUS [8–16], COSY [17–24], GSI [25], and JINR [26]. Whereas initially proton-proton (pp)-induced two-pion production was the primary aim of these measurements [8–15, 17–19], the interest moved later to proton-neutron (pn)-induced reaction channels, after the first clear-cut evidence for a dibaryon resonance with $I(J^P) = 0(3^+)$ had been observed in the $pn \rightarrow d\pi^0\pi^0$ reaction [16, 20, 21]. Subsequent measurements of the $pn \rightarrow d\pi^+\pi^-$ [22], $pn \rightarrow pp\pi^0\pi^-$ [23], $np \rightarrow np\pi^0\pi^0$ [24], and $pn \rightarrow pn\pi^+\pi^-$ [25, 27] reactions revealed that all two-pion production channels, which contain isoscalar contributions, exhibit a signal of this resonance, now called $d^*(2380)$ after observation of its pole in pn scattering [28–30].

Aside from the dibaryon resonance phenomenon the standard theoretical description of the two-pion production process at the energies of interest here is dominated by t -channel meson exchange leading to excitation and decay of the Roper resonance $N^*(1440)$ and of the $\Delta(1232)\Delta(1232)$ system [31, 32]. At lower incident energies the Roper excitation dominates. At incident energies beyond 1 GeV the $\Delta\Delta$ process takes over. Such calculations [31, 32] give quite a reasonable description of the total cross-section data, with the exception of the experimental $pp \rightarrow pp\pi^0\pi^0$ cross section [3, 12, 14] above 1 GeV. After readjusting the decay branching of the Roper resonance used in these calculations to that obtained in recent analyses of data on pion- and photon-induced two-pion production [33, 34], a quantitative description of total and differential cross-section data was achieved for both the $pp \rightarrow pp\pi^0\pi^0$ and the $pp \rightarrow pp\pi^+\pi^-$ reactions at incident energies below 0.9 GeV [8–11, 19], where the Roper excitation dominates.

For a quantitative description of the $pp \rightarrow pp\pi^0\pi^0$ data above 1 GeV, however, the calculation of the $\Delta\Delta$ process as used originally in Ref. [31] had to be modified [14], in particular the ρ -exchange contribution had to be strongly reduced. Also, the strength of the Roper excitation had to be reduced in accord with data and isospin decomposition [12, 14]. In order

to describe the $pp \rightarrow nn\pi^+\pi^+$ reaction quantitatively, too, a contribution from a higher-lying broad Δ resonance, e.g., the $\Delta(1600)$, had to be assumed [15]. These calculations, called now “modified Valencia” calculations give a good description of all data in pp -induced and also of pn -induced channels—if in the latter the $d^*(2380)$ resonance is taken into account—with one striking exception: the $pp \rightarrow pp\pi^+\pi^-$ total cross-section data beyond 0.9 GeV are strongly underpredicted (see dashed line in Fig. 4). This problem was already noted in the isospin decomposition of pp -induced two-pion production [12]. However, since all the $pp \rightarrow pp\pi^+\pi^-$ data beyond 0.8 GeV originate from early low-statistics bubble-chamber measurements, it appears appropriate to reinvestigate this region by exclusive and kinematically complete measurements.

There is yet another point of interest in this reaction at energies above 0.8 GeV. Dyson and Xuong [35] were the first who properly predicted the dibaryon resonances $d^*(2380)$ (called $D_{11} = D_{03}$ by Dyson and Xuong) and D_{12} , the latter denoting a slightly bound ΔN threshold state with $I(J^P) = 1(2^+)$. For a recent discussion about that state see, e.g., Ref. [36] and references therein. According to Dyson and Xuong, as well as to recent Faddeev calculations performed by Gal and Garcilazo [37], there should exist still another ΔN threshold state with $I(J^P) = 2(1^+)$, called D_{21} in Ref. [35]. Very recently also another theoretical study appeared stating that, if existent, D_{21} should have a somewhat larger mass than D_{12} based on the spin-isospin splittings observed for baryons [38].

Because of its large isospin of $I = 2$, this state cannot be excited directly by incident NN collisions, but only associatedly—favorably by production of an additional pion, which carries away one unit of isospin. By isospin selection the decay of an isotensor ΔN state will dominantly proceed into the purely isotensor $pp\pi^+$ channel. Hence the $pp \rightarrow pp\pi^+\pi^-$ reaction is the ideal place to look for the process $pp \rightarrow D_{21}^{++}\pi^- \rightarrow pp\pi^+\pi^-$, as already suggested in Ref. [35]. The main results of this investigation have been communicated recently in a Letter [39].

II. EXPERIMENT

Exclusive and kinematically complete measurements of the $pp \rightarrow pp\pi^+\pi^-$ reaction have been achieved by utilizing the quasifree process in pd collisions. The experiment was carried out with the WASA detector at COSY

(Forschungszentrum Jülich) having a proton beam of energy $T_p = 1.2$ GeV hit a deuterium pellet target [40,41]. By use of the quasifree scattering process $pd \rightarrow pp\pi^+\pi^- + n_{\text{spectator}}$, we can exploit the Fermi motion in the target deuteron and cover thus the energy region $T_p = 1.08$ – 1.36 GeV ($\sqrt{s} = 2.35$ – 2.46 GeV) of the $pp \rightarrow pp\pi^+\pi^-$ reaction.

The analysis used data that were taken with a hardware trigger, which required two charged hits in the forward detector and two charged hits in the central detector. In the off-line analysis the reaction $pd \rightarrow pp\pi^+\pi^- + n$ was selected by requiring two proton tracks in the forward detector in addition to one π^+ and one π^- track in the central detector. The unmeasured neutron four-momentum could be reconstructed that way by a kinematic fit with one overconstraint. The achieved resolution in \sqrt{s} was about 20 MeV.

For the identification of the charged particles registered in the segmented forward detector of WASA we applied the $\Delta E - E$ energy loss method using all combinations of signals stemming from the five layers of the forward range hodoscope. In the central detector the charged particles have been identified by their curved track in the magnetic field as well as by their energy loss in the surrounding plastic scintillator barrel and electromagnetic calorimeter.

The momentum distribution of the reconstructed neutron is shown in Fig. 1. The dashed curve gives the expected momentum distribution for a spectator neutron according to the deuteron wave function based on the CD Bonn potential [42]. Compared to previous measurements on $d\pi^0\pi^0$ [20], $d\pi^+\pi^-$ [22], $np\pi^0\pi^0$ [24], and $pp\pi^0\pi^-$ [23] channels we find here a somewhat enhanced background from nonspectator contributions. In order to keep these background contributions smaller than 2%, we would need to restrict the spectator momentum range to $p < 0.10$ GeV/c. But such a cut would severely reduce the covered energy range to 1.15 GeV $< T_p < 1.3$ GeV (2.38 GeV $< \sqrt{s} < 2.44$ GeV). To reliably evaluate the data up to $p = 0.15$ GeV/c for the quasifree reaction, as done in our previous analyses, we decided to perform a proper background correction by analyzing additionally the nonspectator reaction process by evaluating the data in the nonoverlap region $p_n > 0.25$ GeV/c.

The instrumental acceptance has been 30% in case of the quasifree process and about 5% in case of the nonquasifree reaction due to the requirement that the two protons have to be in the angular range covered by the forward detector and that π^+ and π^- have to be in the angular range of the central detector. The total reconstruction efficiency including all cuts and conditions has been 1.1% for the quasifree process and about 0.2% for the nonquasifree process. In total a sample of about 26 000 events has been selected meeting all cuts and conditions for the quasifree process $pd \rightarrow pp\pi^+\pi^- + n_{\text{spectator}}$. For $p > 0.25$ GeV/c in the region of the nonquasifree process this number is about 20 000.

Efficiency and acceptance corrections of the data have been performed by MC simulations of reaction process and detector setup. For the MC simulations both pure phase-space and model descriptions have been used, which will be discussed below. Since WASA does not cover the full reaction phase space, albeit a large fraction of it, these corrections are not fully model independent. The hatched gray histograms in

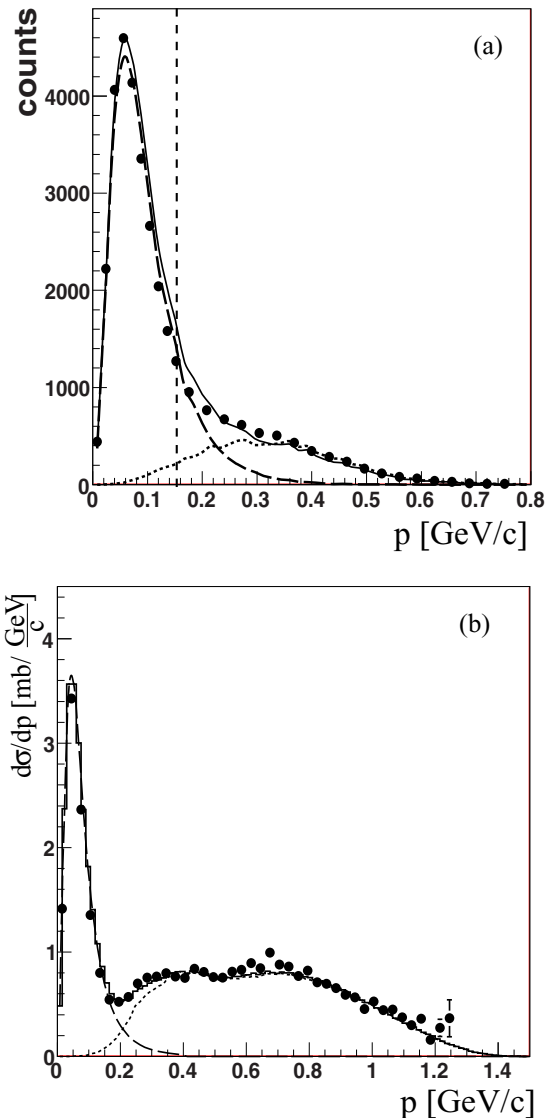


FIG. 1. Distribution of the neutron momenta in the $pd \rightarrow npp\pi^+\pi^-$ reaction (a) before and (b) after acceptance and efficiency correction. Data are given by solid dots. The dashed line shows the expected distribution for the quasifree process $pd \rightarrow pp\pi^+\pi^- + n_{\text{spectator}}$ based on the CD Bonn potential [42] deuteron wave function. The vertical line indicates the region $p < 0.15$ GeV/c used for the evaluation of the quasifree process. The dotted line gives the modeling of the nonquasifree reaction process. The solid line is the incoherent sum of both processes.

Figs. 2, 3 and 5–11 give an estimate for these systematic uncertainties. As a measure of these we have taken the difference between model corrected results and those obtained by assuming pure phase space for the acceptance corrections in case of the nonspectator background reaction. In case of the quasifree $pp \rightarrow pp\pi^+\pi^- + n_{\text{spectator}}$ reaction we use the difference between the results obtained with the final model and those using the modified Valencia model for the acceptance correction. Compared to the uncertainties in these corrections, systematic errors associated with modeling the reconstruction of particles are negligible.

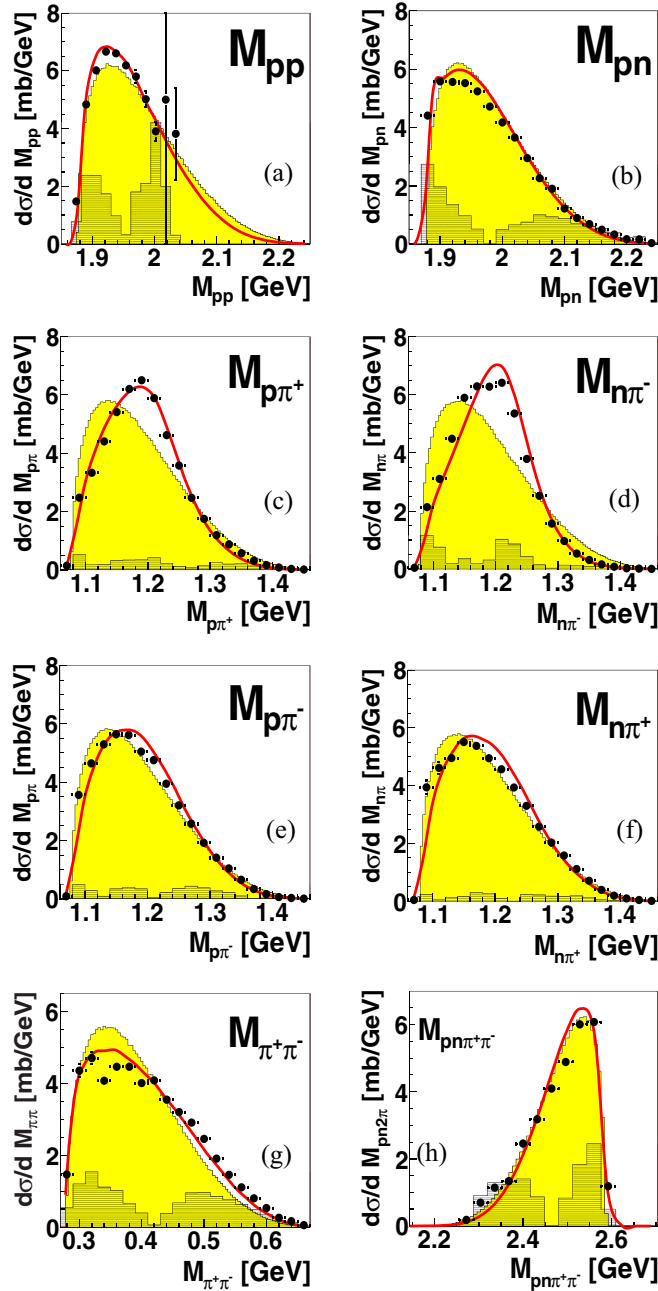


FIG. 2. Differential distributions of the nonspectator background reaction $pd \rightarrow p p n \pi^+ \pi^-$ for the invariant mass distributions (a) M_{pp} , (b) M_{pn} , (c) $M_{p\pi^+}$, (d) $M_{n\pi^-}$, (e) $M_{p\pi^-}$, (f) $M_{n\pi^+}$, (g) $M_{\pi^+\pi^-}$, and (h) $M_{p n \pi^+ \pi^-}$ for $p_n > 0.2$ GeV/c. The shaded areas represent pure phase-space distributions. The hatched areas indicate systematic uncertainties due to the restricted phase-space coverage. The solid curves give a modeling of the process $pd \rightarrow p p n \pi^+ \pi^-$.

The absolute normalization of the data has been obtained by comparing the quasifree single-pion production process $pd \rightarrow p p \pi^0 + n_{\text{spectator}}$ to previous bubble-chamber results for the $pp \rightarrow p p \pi^0$ reaction [3,5]. That way, the uncertainty in the absolute normalization of our data is essentially that of the previous $pp \rightarrow p p \pi^0$ data, i.e., in the order of 5–15%.

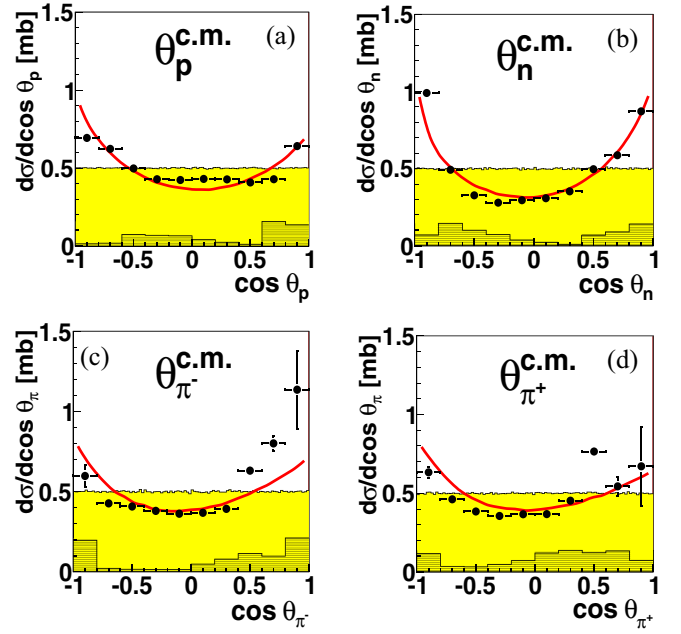


FIG. 3. Same as Fig. 2, but for the angular distributions of (a) protons ($\Theta_p^{c.m.}$), (b) neutrons ($\Theta_n^{c.m.}$), (c) positive pions ($\Theta_{\pi^-}^{c.m.}$), and (d) negative pions ($\Theta_{\pi^+}^{c.m.}$).

III. NONSPECTATOR BACKGROUND PROCESS

$$pd \rightarrow p p n \pi^+ \pi^-$$

The nonspectator background process $pd \rightarrow p p n \pi^+ \pi^-$ was selected by a cut on the neutron momentum $p_n > 0.25$ GeV/c. For an axially symmetric five-body final state there are eleven independent differential observables. For the nonspectator background reaction $pd \rightarrow p p n \pi^+ \pi^-$ we show in Figs. 2(a)–2(h) and 3(a)–3(d) twelve differential observables: the invariant mass distributions M_{pp} , M_{pn} , $M_{p\pi^+}$, $M_{n\pi^-}$, $M_{p\pi^-}$, $M_{n\pi^+}$, $M_{\pi^+\pi^-}$, and $M_{p n \pi^+ \pi^-}$ as well as the angular distributions for protons ($\Theta_p^{c.m.}$), neutrons ($\Theta_n^{c.m.}$), positive pions ($\Theta_{\pi^-}^{c.m.}$), and negative pions ($\Theta_{\pi^+}^{c.m.}$).

The obtained differential distributions deviate partly substantially from pure phase-space distributions. This is the case in particular for the distributions of the invariant masses $M_{p\pi^+}$ and $M_{n\pi^-}$ exhibiting the excitations of Δ^{++} and Δ^- , as well as of the angles $\Theta_p^{c.m.}$, $\Theta_n^{c.m.}$, $\Theta_{\pi^-}^{c.m.}$ and $\Theta_{\pi^+}^{c.m.}$. However, all differential distributions fit well to a modeling of the process $pd \rightarrow N \Delta \Delta \rightarrow p p n \pi^+ \pi^-$. Since it proceeds dominantly via the $\Delta^{++} \Delta^-$ configuration due to isospin selection, the $M_{p\pi^+}$ and $M_{n\pi^-}$ spectra peak at the Δ mass, as we observe in Fig. 2. The pion angular distributions are as expected from the p -wave decay of the intermediate Δ resonances. Proton and neutron angular distributions are strongly curved as expected from a peripheral collision. In comparison to the neutron angular distribution, the proton angular distribution appears to be less anisotropic, since only one of the two protons is dominantly active.

The success of such a background modeling is of no great surprise, since the $p n \pi^+ \pi^-$ channel has the by far largest two-pion production cross section. Also we know from the $pd \rightarrow {}^3\text{He} p \pi$ reaction, where the $p p n$ system has fused to

${}^3\text{He}$, that for $T_p > 1$ GeV the t -channel $\Delta\Delta$ process is by far dominating [43]. As in the latter case we observe also here the Δ signals in the invariant mass spectra to be somewhat broadened, which may be traced back to the Fermi motion of the participating nucleons and may be accounted for most easily by increasing the Δ width from 120 MeV to 140 MeV by a fit to the data.

Having achieved a quantitative description of the non-quasifree background process for $p_n > 0.25$ GeV/ c , we may extrapolate its contribution reliably also for $p_n < 0.15$ GeV/ c and subtract it from the measured neutron momentum distribution (Fig. 1), in order to obtain the pure quasifree part, which is of main interest here.

IV. QUASIFREE REACTION $pp \rightarrow pp\pi^+\pi^- + n_{\text{spectator}}$

A. Total cross section

For the determination of the energy dependence of total and differential cross sections we have divided the background subtracted data for the quasifree process into bins of 50 MeV width in the incident energy T_p . The resulting total cross sections are shown in Fig. 4, top (solid dots), together with results from earlier measurements (other symbols) [2–4,8–10,19]. Our data are in reasonable agreement with the earlier measurements in the overlap energy region.

The $pp \rightarrow pp\pi^+\pi^-$ data exhibit a smoothly and monotonically rising cross section, in contrast to the situation in the closely related $pp\pi^0\pi^0$ channel, where the experimental cross section flattens out above 0.9 GeV followed by renewed rise above 1.2 GeV, see Fig. 4, bottom. This different behavior of both channels is discussed in the following.

For comparison to theoretical expectations we first plot in Fig. 4 the results of the original Valencia calculations [31] by the short-dashed lines. At first glance the agreement with the data for the $pp\pi^+\pi^-$ channel appears remarkable, though they predict about 40% larger cross sections in the region of our measurements. However, as mentioned already in Sec. I, these calculations are far off for the $pp\pi^0\pi^0$ channel, as illustrated in the bottom panel of Fig. 4.

The experimental $pp\pi^0\pi^0$ cross section exhibits a quite flat energy dependence in the energy range $T_p = 0.9$ –1.2 GeV. Thereafter it starts rising again producing thus a kind of kink structure around 1.2 GeV. This behavior is observed both in the WASA measurements [12,14] as well as in the previous KEK bubble-chamber measurements [3]. As demonstrated by isospin decomposition [12] of the various two-pion production channels, the behavior observed in the $pp\pi^0\pi^0$ channel can be traced back to the dominance of the Roper excitation at low incident energies followed by that of the $\Delta\Delta$ process at higher energies.

After readjusting the decay branchings of the Roper resonance used in the original Valencia calculations to those obtained in recent analyses of pion- and photon-induced two-pion production data [33,34] and by retuning the $\Delta\Delta$ process [14] a quantitative description of the total and in particular also of the differential cross-section data was achieved for the $pp \rightarrow pp\pi^0\pi^0$ reaction [11,14]. These so-called modified Valencia calculations are shown in Fig. 4 by the long-dashed

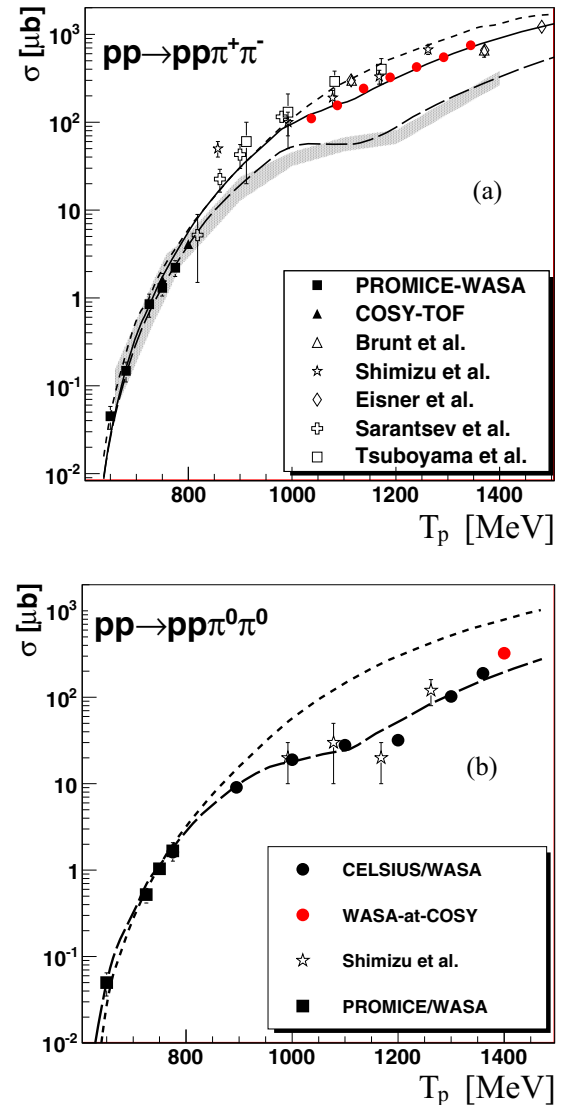


FIG. 4. Total cross section in dependence of the incident proton energy T_p for the reactions (a) $pp \rightarrow pp\pi^+\pi^-$ and (b) $pp \rightarrow pp\pi^0\pi^0$. The solid dots in (a) show results from this work. Solid symbols in (b) display WASA results at different installations [9,12,17]. Other symbols denote results from previous experiments [2–4,8–10,19]. The short-dashed lines give the original Valencia calculation [31], the long-dashed ones the so-called modified Valencia calculation [14]. The solid line is obtained, if to the latter an associatedly produced D_{21} resonance is added according to the process $pp \rightarrow D_{21}\pi^- \rightarrow pp\pi^+\pi^-$ with the strength of this process being fitted to the total cross section data. The grey shaded band exhibits the results of Eq. (1) based on the $pp\pi^0\pi^0$ channel.

lines both for the $pp\pi^+\pi^-$ (top) and the $pp\pi^0\pi^0$ channel (bottom).

These modified Valencia calculations do also very well for the $pp\pi^+\pi^-$ channel at low energies both for the total (Fig. 4, top) and the differential cross sections [19], but yield a much too low cross section at higher energies. The reason for this failure is that by isospin relations the energy dependences of $pp\pi^0\pi^0$ and $pp\pi^+\pi^-$ channels have to be qualitatively

similar, if only t -channel Roper and $\Delta\Delta$ processes contribute. In that case the matrix element $M_{I_{pp}^f I_{\pi\pi}^f I_{pp}^f} = M_{111}$ (ρ channel in the $\pi^+\pi^-$ subsystem) vanishes [12,44].¹ So, if the kink around $T_p \approx 1.2$ GeV in the $pp\pi^0\pi^0$ data [14] got to be reproduced by such model calculations, then also the $pp\pi^+\pi^-$ channel has to behave similarly, if only these two processes are at work.

In the total cross section the t -channel Roper and $\Delta\Delta$ excitations interfere only weakly (see, e.g., Fig. 3 in Ref. [31], where the cross sections of the individual processes are seen to just add up in good approximation), since both excitations act on quite different phase-space volumes. Hence we may neglect their interference in good approximation and obtain thus from isospin decomposition, Eqs. (1)–(5) in Ref. [12] for the total cross sections of $pp\pi^0\pi^0$ and $pp\pi^+\pi^-$ channels:

$$\begin{aligned}\sigma_{pp\pi^0\pi^0} &\approx \sigma^{N^*} + \sigma^{\Delta\Delta} \\ \sigma_{pp\pi^+\pi^-} &\approx 2\sigma^{N^*} + \frac{9}{8}\sigma^{\Delta\Delta} + \frac{1}{8}|M_{111}|^2,\end{aligned}\quad (1)$$

where σ^{N^*} and $\sigma^{\Delta\Delta}$ denote the cross sections of t -channel Roper and $\Delta\Delta$ processes, respectively. Since the relative weight of the $\Delta\Delta$ process is less than that of the Roper process in $\sigma_{pp\pi^+\pi^-}$, the kink near $T_p \approx 1.2$ GeV is smaller than in $\sigma_{pp\pi^0\pi^0}$, but still present, because the $\Delta\Delta$ process provides a much bigger cross section than the Roper process does. In Fig. 4, top, the isospin-based prediction according to Eq. (1) is plotted by the gray shaded band. At low energies it agrees perfectly with the modified Valencia calculation, which was tuned to the data in the $pp\pi^0\pi^0$ channel. At higher energies the band deviates slightly from the model calculation. The reason for this is that the model calculation includes interference between Roper and $\Delta\Delta$ processes, which is neglected in the isospin result, and also includes contributions from $\Delta(1600)$ not included in the isospin-based result.

We note in passing that in the article about isospin decomposition [12] the missing strength in the $pp\pi^+\pi^-$ channel appeared still less dramatic, since at that time full interference between the isospin matrix elements for Roper and $\Delta\Delta$ excitations was assumed. But as later model calculations showed, this interference is very small. For that reason interferences between the various resonance excitations have been omitted completely in the model calculations of Ref. [32].

The $\Delta(1600)$ excitation also contributes to M_{111} albeit much too little in order to heal the deficit in the cross section. The modified Valencia calculations (dashed line in Fig. 4) do include this contribution.

In this context we also have to ask whether possibly other higher-lying N^* and Δ resonances provide substantial contributions in the energy region of interest here. This has been comprehensively investigated in Ref. [32] with the result that all of these [including also $N^*(1520)$] give only negligible contributions to the two-pion production cross sections.

B. Differential cross sections

The differential distributions do not exhibit any particularly strong energy dependence in their shapes, when binned into T_p bins of 50 MeV width, which is of no surprise, since the energy region covered in this measurement is dominated by $\Delta\Delta$ and Roper excitations with very smooth energy dependences due to their large decay widths. Hence we discuss the differential distributions at first unbinned, i.e., averaged over the full covered energy range.

For an axially symmetric four-body final state there are seven independent differential observables. But for a better understanding of the underlying physics we decided to show more, namely nine differential distributions. These are the ones for the center-of-mass (c.m.) angles for protons and pions denoted by $\Theta_p^{c.m.}$, $\Theta_{\pi^+}^{c.m.}$, and $\Theta_{\pi^-}^{c.m.}$, respectively, as well as those for the invariant masses M_{pp} , $M_{\pi^+\pi^-}$, $M_{p\pi^+}$, $M_{pp\pi^+}$, $M_{p\pi^-}$ and $M_{pp\pi^-}$. These distributions are shown in Figs. 5(a)–5(f) and 6(a)–6(c).

There are no data to compare with from previous experiments in the energy range considered here. Except for $\Theta_{\pi^-}^{c.m.}$ all measured differential distributions differ markedly in shape from pure phase-space distributions (shaded areas in Figs. 5–6). With the exception of $\Theta_{\pi^+}^{c.m.}$, $M_{p\pi^-}$, and $M_{pp\pi^-}$ spectra, the differential distributions are reasonably well reproduced by the modified Valencia model calculations (long-dashed curves). For the original Valencia calculation (short-dashed lines), which contains substantial contributions from the Roper excitation still in this energy region, large discrepancies get apparent in addition for the $M_{\pi^+\pi^-}$ and $\Theta_p^{c.m.}$ distributions. For better comparison all calculations are adjusted in area to the data in Figs. 5–11.

Because of identical particles in the entrance channel all c.m. angular distributions have to be symmetric about 90° . Within uncertainties this requirement is met by the data. The proton angular distribution is forward-backward peaked as expected for a peripheral reaction process. The π^- angular distribution is flat, in tendency slightly convex curved as also observed in the other $NN\pi\pi$ channels at these energies. But surprisingly, the π^+ angular distribution exhibits a strikingly concave shape. Such a strange behavior, which is in sharp contrast to the theoretical expectation, has been observed so far in none of the two-pion production channels.

Also the $M_{p\pi^-}$ spectrum is markedly different from the $M_{p\pi^+}$ spectrum. The same is true for the $M_{pp\pi^-}$ spectrum with respect to the $M_{pp\pi^+}$ distribution. In case of the t -channel $\Delta\Delta$ process, which is thought to be the dominating one at the energies of interest here, Δ^{++} and Δ^0 get excited simultaneously and with equal strengths. Hence, the $M_{p\pi^+}$ ($M_{pp\pi^+}$) spectrum should be equal to the $M_{p\pi^-}$ ($M_{pp\pi^-}$) one and also the π^+ angular distribution should be identical to the π^- angular distribution. So the failure of the modified Valencia calculation to describe properly the total cross section and the differential distributions underlines the suspicion that the t -channel $\Delta\Delta$ process is not the leading process here.

Since the total cross section is grossly underpredicted above $T_p \approx 1.0$ GeV, it appears that an important piece of reaction dynamics is missing, which selectively affects the $pp\pi^+\pi^-$ channel. Furthermore, the discrepancy between data and modified Valencia description opens up scissorlike around

¹Neglecting a very small contribution from the Roper decay branch $N^* \rightarrow \Delta\pi$.

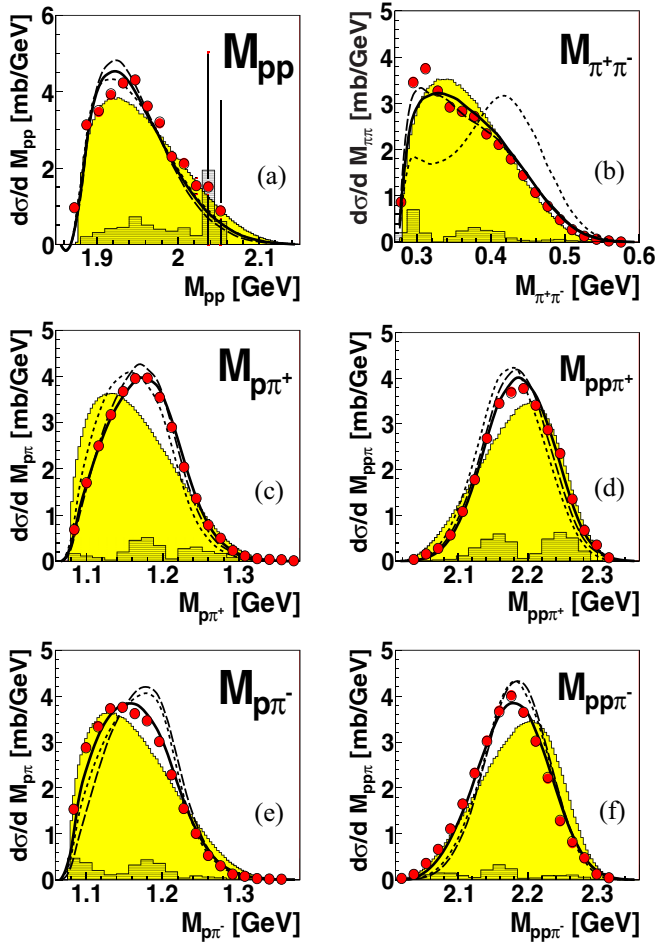


FIG. 5. Differential distributions of the $pp \rightarrow pp\pi^+\pi^-$ reaction in the region $T_p = 1.08\text{--}1.36$ GeV for the invariant-masses (a) M_{pp} , (b) $M_{\pi^+\pi^-}$, (c) $M_{p\pi^+}$, (d) $M_{pp\pi^+}$, (e) $M_{p\pi^-}$ and (f) $M_{pp\pi^-}$. Filled (open) circles denote the results from this work after (before) background subtraction. In most cases these symbols lie on top of each other. The hatched histograms indicate systematic uncertainties due to the restricted phase-space coverage of the data. The shaded areas represent pure phase-space distributions, short-dashed (long-dashed) lines represent original (modified) Valencia calculations [31] ([14]). The solid lines include the process $pp \rightarrow D_{21}\pi^- \rightarrow pp\pi^+\pi^-$. All calculations are normalized in area to the data.

$T_p \approx 0.9$ GeV, which suggests the opening of a new channel, where a ΔN system is produced associatedly with another pion. Such a state with the desired properties could be the isotensor D_{21} state with $I(J^P) = 2(1^+)$ predicted already by Dyson and Xuong [35] with a mass close to that of its isospin partner D_{12} with $I(J^P) = 1(2^+)$. Whereas D_{12} can be reached directly by the initial pp channel, D_{21} cannot be reached that way because of its isospin $I = 2$. However, it can be produced in initial pp collisions associatedly with an additional pion.

C. D_{12} resonance

In several partial-wave analyses of pp and πd scattering as well as of the $pp \rightarrow d\pi^+$ reaction the D_{12} resonance has

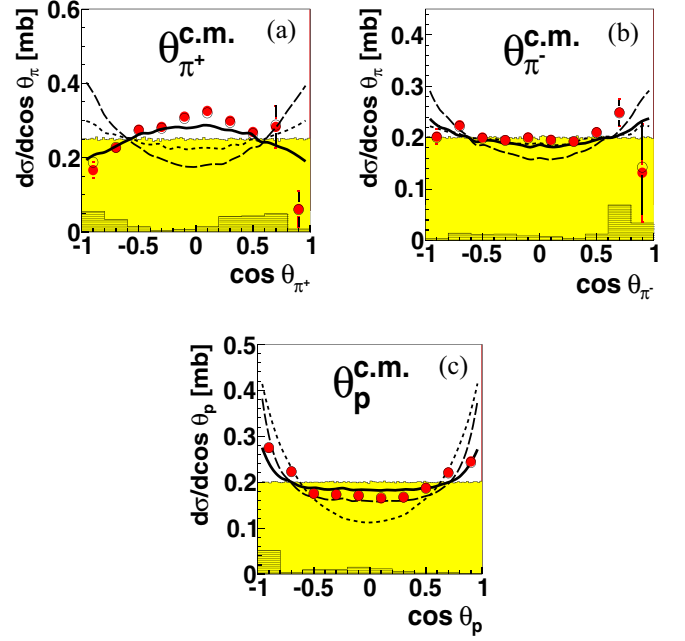


FIG. 6. The same as Fig. 5, but for the c.m. angles of positive and negative pions (a) $\Theta_{\pi^+}^{c.m.}$ and (b) $\Theta_{\pi^-}^{c.m.}$, respectively, as well as protons (c) $\Theta_p^{c.m.}$.

been identified at a mass of 2144–2148 MeV [45,46], i.e., with a binding energy of a few MeV relative to the nominal ΔN threshold, and with a width compatible to that of the Δ resonance. For a recent discussion about the nature of this D_{12} state see, e.g., Ref. [36] and references therein. Also recent Faddeev calculations for the $NN\pi$ system find both D_{12} and D_{21} dibaryon resonances with masses slightly below the ΔN threshold and with widths close to that of the Δ resonance [37]. The decay of the D_{12} resonance proceeds dominantly into $d\pi$ and $np\pi$ channels, since there the np pair can reside in the 3S_1 partial wave, which readily couples with the p -wave pion (from Δ decay) to $J^P = 2^+$. In contrast, its decay into $pp\pi$ is heavily suppressed, since the pp pair can couple only to 1S_0 in relative s wave and hence needs at least relative d waves for building a $J^P = 2^+$ state in the $pp\pi$ system. Since it does not show up in the $pp\pi$ system, it also will not appear in the $pp \rightarrow pp\pi^+\pi^-$ reaction.

D. D_{21} resonance

The hypothetical isotensor state D_{21} , on the other hand, strongly favors the purely isotensor channel $pp\pi^+$ in its decay. In addition, $J^P = 1^+$ can be easily reached by adding a p -wave pion (from Δ decay) to a pp pair in the 1S_0 partial wave. Hence, as already suggested by Dyson and Xuong [35], the favored production process should be in the $pp \rightarrow pp\pi^+\pi^-$ reaction.

If we use the formalism outlined in Ref. [47], then the resonance process $pp \rightarrow D_{21}\pi \rightarrow \Delta p\pi \rightarrow pp\pi\pi$ can be described by the transition amplitude

$$M_R(m_{p_1}, m_{p_2}, m_{p_3}, m_{p_4}, \hat{k}_1, \hat{k}_2) = M_R^0 \Theta_R(m_{p_1}, m_{p_2}, m_{p_3}, m_{p_4}, \hat{k}_1, \hat{k}_2), \quad (2)$$

where the function Θ contains the substate and angular-dependent part, and

$$M_R^0 = D_{D_{21}} * D_\Delta \quad (3)$$

with $D_{D_{21}}$ and D_Δ denoting the corresponding resonance propagators. Here p_1 , p_2 and p_3 , p_4 denote the ingoing and outgoing protons, respectively. k_1 is the momentum of the associatedly produced pion and k_2 that of the pion resulting from the decay $D_{21} \rightarrow \Delta p \rightarrow pp\pi$.

If the coordinate system is chosen to be the standard one with the z axis pointing in beam direction [implying $m_L = 0$ and $(\Theta_i, \Phi_i) = (0, 0)$], then the function $\Theta_R(m_{p_1}, m_{p_2}, m_{p_3}, m_{p_4}, \hat{k}_1, \hat{k}_2)$ defined in Eq. (2) is built up by the corresponding vector-coupling coefficients and spherical harmonics representing the angular dependence due to the orbital angular momenta involved in the reaction:

$$\begin{aligned} & \Theta_R(m_{p_1}, m_{p_2}, m_{p_3}, m_{p_4}, \hat{k}_1, \hat{k}_2) \\ &= \sum \left(\frac{1}{2} \frac{1}{2} m_{p_1} m_{p_2} \left| S m_s \right. \right) (SLm_s 0 | JM) \\ & \times (JM | J_{D_{21}} l m_{D_{21}} m_1) \left(J_{D_{21}} m_{D_{21}} \left| \frac{3}{2} \frac{1}{2} m_\Delta m_{p_3} \right. \right) \\ & \times \left(\frac{3}{2} m_\Delta \left| \frac{1}{2} 1 m_{p_4} m_2 \right. \right) Y_{L_0}(0, 0) Y_{l m_1}(\hat{k}_1) Y_{l m_2}(\hat{k}_2). \end{aligned} \quad (4)$$

The D_{21} resonance can be formed together with an associatedly produced pion either in relative s or p wave. In the first instance the initial pp partial wave is 3P_1 , in the latter one it is 1S_0 or 1D_2 . The first case is special, since here $(SL00 | JM) = (1100 | 10) = 0$. Only in this case Eq. (4) yields a $\sin\Theta_\pi$ dependence for the angular distribution of the pion originating from the D_{21} decay, exactly what is needed for the description of the data for the π^+ angular distribution.

In fact, if we add such a resonance with the processes

$$\begin{aligned} pp &\rightarrow D_{21}^{++\pi^-} \rightarrow \Delta^{++} p \pi^- \rightarrow pp\pi^+\pi^- \\ pp &\rightarrow D_{21}^+\pi^+ \rightarrow \Delta^0 p \pi^+ \rightarrow pp\pi^+\pi^- \end{aligned} \quad (5)$$

with fitted mass $m_{D_{21}} = 2140$ MeV and width $\Gamma_{D_{21}} = 110$ MeV, we obtain a good description of the total cross section by adjusting the strength of the assumed resonance process to the total cross-section data (solid line in Fig. 4). Simultaneously, the addition of this resonance process provides a quantitative description of all differential distributions (solid lines in Figs. 5–11), in particular also of the $\Theta_{\pi^+}^{c.m.}$, $M_{p\pi^-}$, and $M_{pp\pi^-}$ distributions. Due to isospin coupling the branch via Δ^0 is very small and yields only marginal contributions to the observables. Since therefore the D_{21} decay populates practically only Δ^{++} , its reflexion in the $M_{p\pi^-}$ spectrum shifts the strength to lower masses, as required by the data. The same holds for the $M_{pp\pi^-}$ spectrum. We are not aware of any other mechanism that could provide an equally successful description of the observables of the $pp \rightarrow pp\pi^+\pi^-$ reaction at the energies of interest here.

We note that the only other place in pion production, where a concave curved pion angular distribution has been observed, is the $pp \rightarrow pp\pi^0$ reaction in the region of single

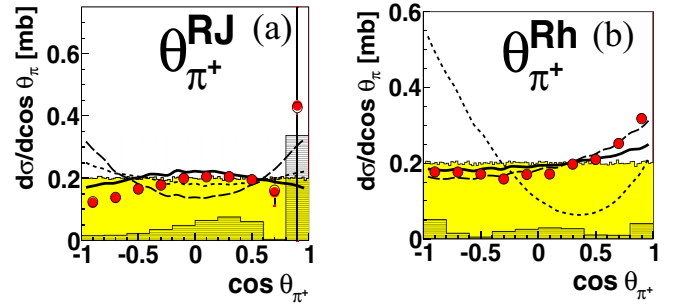


FIG. 7. The same as Fig. 6, but for the angles of positive pions in the D_{21} resonance subsystem either in (a) the Jackson frame ($\Theta_{\pi^+}^{RJ}$) or in (b) the helicity frame ($\Theta_{\pi^+}^{Rh}$).

Δ excitation [48–52]. Also in this case it turned out that the reason was the excitation of resonances in the ΔN system [52] causing a proton spin-flip situation. In general, t -channel resonance excitations are connected with pions emerging in s or p waves in non-spin-flip configurations and hence lead to flat-to-convex shaped angular distributions.

Also the description of the π^- angular distribution improves by inclusion of the D_{21} resonance scenario. Whereas the modified Valencia calculations predict still a distribution, which is significantly convex, the full calculations, which include the D_{21} reaction amplitude with π^- particles emerging in relative s wave, predict a much flatter angular distribution in agreement with the measurements.

1. D_{21} subsystem representations

Next, we look at the differential distributions in the subsystem of interest here, namely the D_{21} resonance system. Since the width of the Δ excitation is not small compared to the available phase-space energy range, the Dalitz plot of invariant masses in the resonance subsystem is just overwhelmingly dominated by the Δ^{++} excitation as already seen in its square-root projections displayed in Fig. 5. Hence we do not need to show the Dalitz plot here. However, since the π^+ angular distribution turned out to be special in the overall center-of-mass system, we look at it once more in the resonance subsystem by plotting it both in the Jackson and in the helicity frame [53] in Figs. 7(a)–7(b).

In the Jackson frame the reference axis for the polar angle $\Theta_{\pi^+}^{RJ}$ is still the beam axis, i.e., the same as in the center-of-mass system. That way entrance- and exit-channel systems stay connected in this representation. Since in addition resonance and center-of-mass systems deviate only by the additional π^- , the mass of which is small compared to the residual mass of the other ejectiles, the angular distributions in these two frames are very similar.

The situation is very different in the helicity frame, where the reference axis for the polar angle $\Theta_{\pi^+}^{Rh}$ is given by the direction of the π^- momentum in the resonance subsystem. Thus this reference frame has no longer a connection to the initial system and is only based on the emitted particles representing the opening angle between the two pions in the resonance frame. In consequence the information about the proton spin flip during the production process is absent in

this representation and with it the sinus shape for the D_{21} contribution. Instead, the D_{21} contribution is flat in this case, since the resonance is in relative s wave with the associated produced π^- particle and hence the directions of the two pions originating from two different sources appear to be uncorrelated. The situation is more complex for the background of conventional t -channel processes. For the $\Delta\Delta$ process the emerging pions originate again from two different largely uncorrelated sources, since the well-known conventional ABC effect causing large $\pi\pi$ correlations and giving rise to an enhancement near $\cos\Theta_{\pi^+}^{Rh} = 1$ (and at low masses in the $M_{\pi\pi}$ spectrum) is only substantial if the nucleons in the exit channel are bound in a nucleus [47,54]. In contrast, the t -channel excitation and decay of the Roper resonance produces a highly correlated pion pair originating from the same source. Hence the distribution of the $\pi\pi$ opening angle is strongly anisotropic [11,14] in this case. And since in the original Valencia model the Roper process is assumed to be still large at the energies of interest here, this calculation predicts a very anisotropic distribution for the helicity angle $\Theta_{\pi^+}^{Rh}$ [short-dashed line in Fig. 7(b)].

Whereas the original Valencia calculations (short-dashed lines in Fig. 7) are grossly at variance with the data in both reference frames, the calculations including the D_{21} resonance process (solid lines) give a good description of the data both in the Jackson and in the helicity frame. For the modified Valencia calculations the situation is split. Whereas they are again at variance with the data in the Jackson frame, they fit even perfect to the data in the helicity frame, in particular at small angles, i.e., near $\cos\Theta_{\pi^+}^{Rh} = 1$, where the data show a slight enhancement. This enhancement in the opening angle is strictly correlated with a corresponding enhancement in the $M_{\pi^+\pi^-}$ distribution at low masses constituting the ABC effect. Though this enhancement is small (see Fig. 5, top right) it is not fully accounted for by the modified Valencia calculations, as already apparent in the analysis of the $pp \rightarrow pp\pi^0\pi^0$ reaction (Fig. 2 in Ref. [14]). So the small failure of the model calculation including the D_{21} resonance to describe the ABC enhancement quantitatively could be traced back to the fact that the background description by the modified Valencia model is not perfect in the ABC effect region.

2. Δ subsystem representation

We now want to check, whether the concave shape of the π^+ angular distribution really originates from Δ excitation and decay associated with a proton spin flip. For this purpose we boost the distribution farther from the D_{21} into the Δ reference frame, see Fig. 8. The concave shape persists also in this case though somewhat washed out due to the fact that we do not know, which of the two emerging protons originates from the Δ . The pure D_{21} process gives a sinus-shaped distribution due to the proton spin flip in the Δ excitation and decay process, whereas the convex shaped results from original (short-dashed) and modified (long-dashed) Valencia calculations provide a convex distribution due to the dominance of the cosine-shaped non-spin-flip Δ process. The original Valencia calculation is less anisotropic than the modified one, since in the former the Roper process providing a flat angular

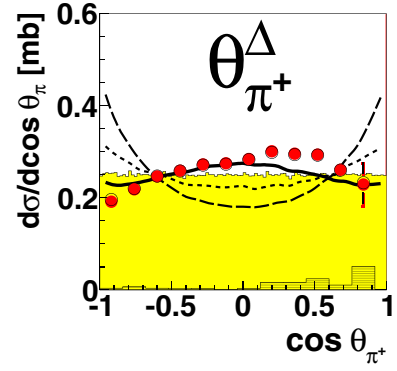


FIG. 8. The same as Fig. 6, but for the angles of positive pions in the Δ resonance subsystem.

dependence plays a larger role. That way, we have traced back the origin of the concave shape of the π^+ -distribution to the proton spin flip in the Δ process as required for the D_{21} production process.

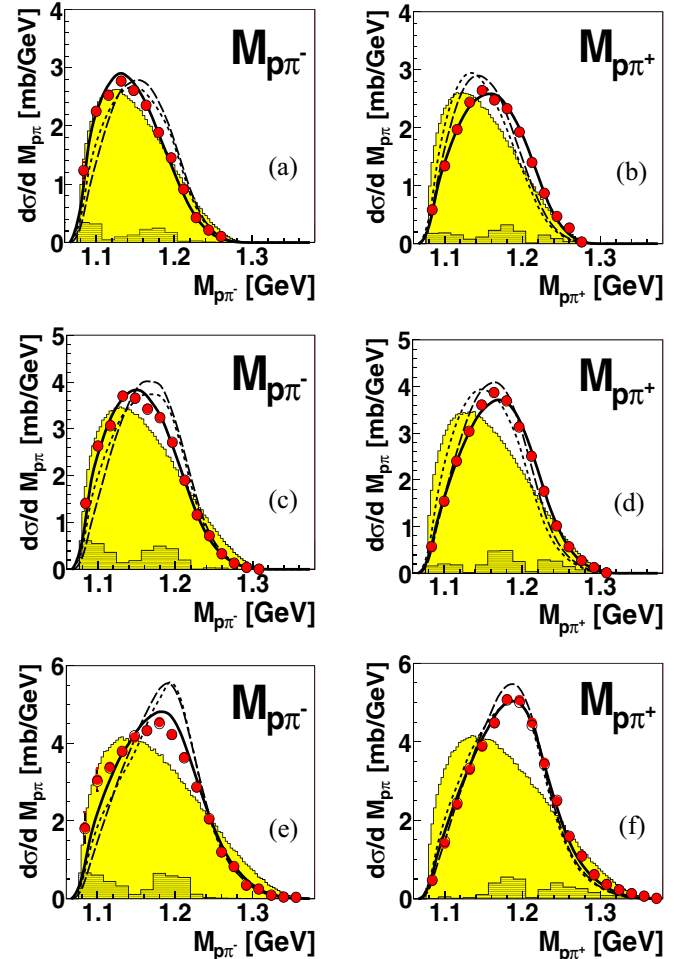


FIG. 9. Same as Fig. 5, but for the differential distributions of the invariant masses $M_{p\pi^-}$ (left) and $M_{p\pi^+}$ (right) for the energy bins at $T_p = 1.10$ (top), 1.18 (middle), and 1.31 GeV (bottom).

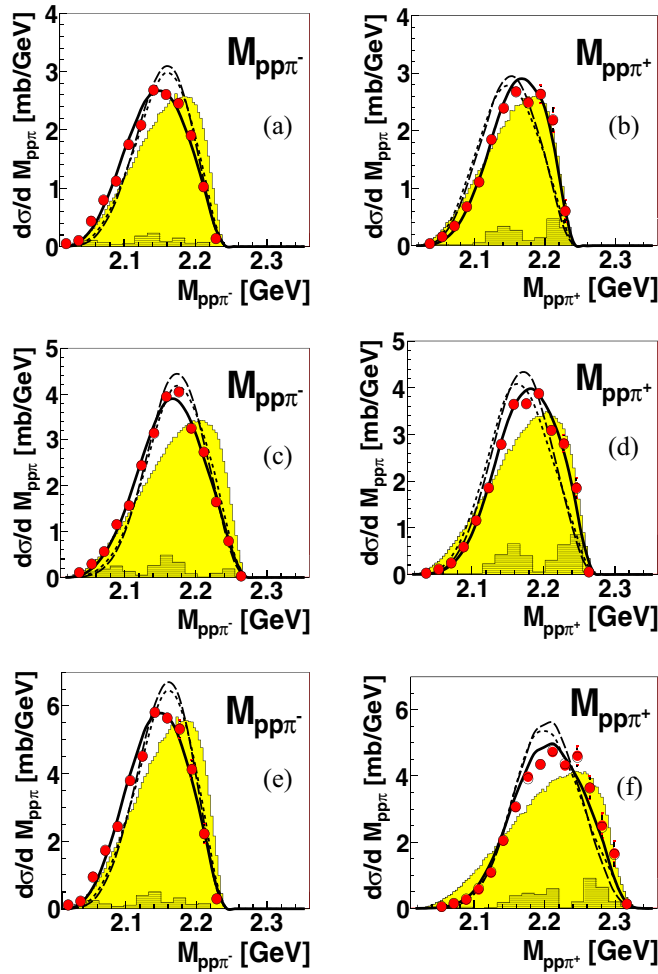


FIG. 10. Same as Fig. 5, but for the differential distributions of the invariant masses $M_{pp\pi^-}$ (left) and $M_{pp\pi^+}$ (right) for the energy bins at $T_p = 1.10$ (top), 1.18 (middle), and 1.31 GeV (bottom).

E. Energy dependence of differential distributions

At the low-energy side of the beam-energy interval covered by our data the D_{21} resonance contributes nearly 60% to the total cross section shrinking slightly to less than 50% at the high-energy end. Hence we expect to observe no substantial changes in the differential distributions of $\Theta_{\pi^+}^{c.m.}$, $M_{p\pi^-}$, and $M_{pp\pi^-}$, just a smooth transition from a more to a somewhat less D_{21} -dominated scenario. In Figs. 9(a)–9(f) to 11(a)–11(f) we plot the three crucial distributions together with their counterparts for the bins at lowest, central, and highest energy. For the π^+ angular distribution we show also their D_{21} resonance subsystem representations for the three energy bins in Figs. 12(a)–12(f).

Indeed, we observe no significant changes, just a smooth transition of strength to higher masses in the $M_{p\pi}$ and $M_{pp\pi}$ spectra. Simultaneously we observe for the $\Theta_{\pi^+}^{c.m.}$ distribution the transition from a pronounced concave shape at the low-energy bin to a slightly flatter distribution at the high-energy bin. The observed smooth energy dependence of differential distributions is in accord with the D_{21} hypothesis (solid lines in Figs. 9–12). Unfortunately, there are no such data available

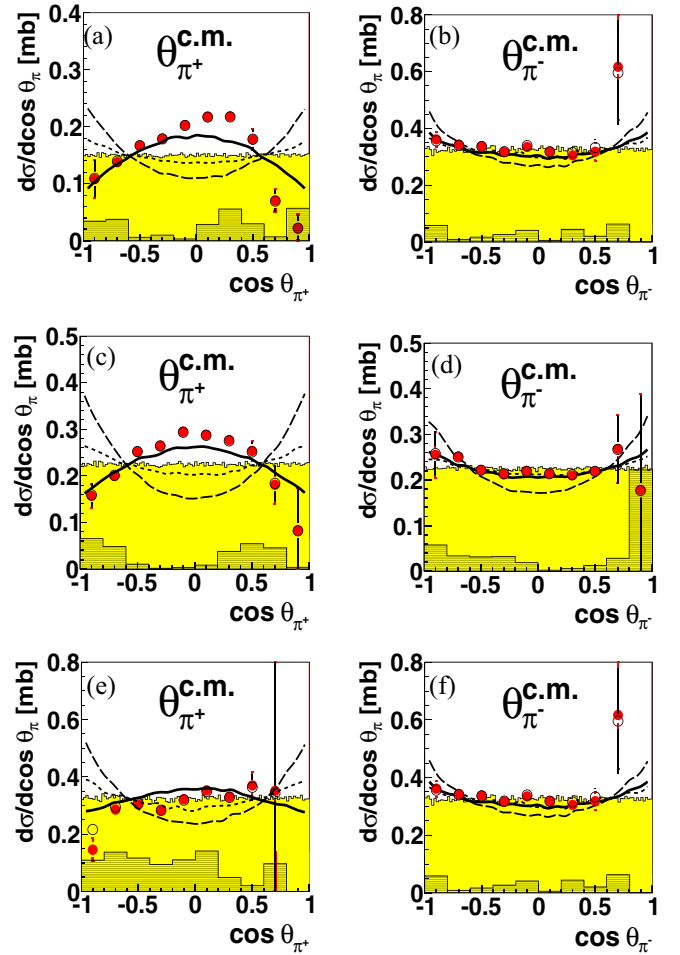


FIG. 11. Same as Fig. 5, but for the differential distributions of the pion angles $\Theta_{\pi^+}^{c.m.}$ (left) and $\Theta_{\pi^-}^{c.m.}$ (right) for the energy bins at $T_p = 1.10$ (top), 1.18 (middle), and 1.31 GeV (bottom).

for the energy region $T_p = 0.9$ – 1.0 GeV, where due to the opening of the D_{21} channel the changes in these spectra are expected to be much bigger.

If this scenario is correct, then the D_{21} contribution of nearly 50% should also persist to higher energies and impress its specific features on the differential observables. Though there are no high-statistics data, there exist at least two bubble-chamber measurements at $T_p = 1.37$ [2] and 2.0 GeV [6], which show a few differential distributions. Despite limited statistics their $M_{p\pi^+}$ and $M_{p\pi^-}$ spectra clearly exhibit the same trend as we observe, namely, a strongly excited Δ^{++} resonance in combination with a much reduced Δ^0 excitation.

F. Resume

As we have demonstrated, the addition of an isotensor dibaryon resonance is able to settle the shortcomings of the modified Valencia calculations for the $pp \rightarrow pp\pi^+\pi^-$ reaction. However, before we can take this as evidence for the existence of an isotensor ΔN resonance, we have to investigate whether this dibaryon hypothesis leads to inconsistencies in the description of other two-pion production

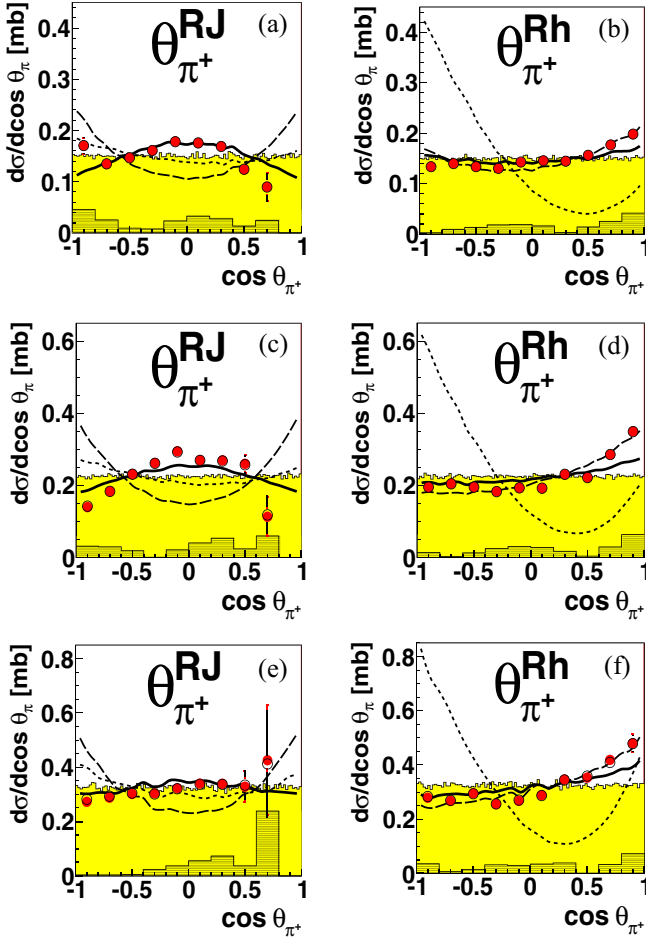


FIG. 12. Same as Fig. 5, but for the angles of positive pions in the D_{21} resonance subsystem either in the Jackson frame ($\Theta_{\pi^+}^{RJ}$, left) or in the helicity frame ($\Theta_{\pi^+}^{Rh}$, right) for the energy bins at $T_p = 1.10$ (top), 1.18 (middle), and 1.31 GeV (bottom).

channels. The reason is that such a state may decay also into $NN\pi$ channels other than the $pp\pi^+$ channel, albeit with much reduced branchings due to their much inferior isospin couplings. Consequently, such a resonance may also contribute to other two-pion production channels. In particular we have to consider, whether it can affect the $pp \rightarrow pp\pi^0\pi^0$ reaction with its comparatively small cross section at the energies of interest here. However, the D_{21} production via the 3P_1 partial wave leaves the two emitted pions in relative p wave to each other. Therefore they must be in an isovector state by Bose symmetry. Such a ρ -channel situation is not possible for identical pions in line with the isospin relations for the various two-pion production channels. Hence there are no contributions from D_{21} in $pp\pi^0\pi^0$ and $nn\pi^+\pi^+$ channels, i.e., there is no consistency problem.

From a fit to the data we obtain a mass $m_{D_{21}} = 2140(10)$ MeV and a width $\Gamma_{D_{21}} = 110(10)$ MeV. The mass is in good agreement with the prediction of Dyson and Xuong [35]. From their Faddeev calculations Gal and Garcilazo [37] obtain slightly larger values for mass and width. Within uncertainties the extracted mass and width of the D_{21} state

coincide with those for the D_{12} state. This means that the masses of this dibaryon doublet do not exhibit any particular isospin dependence, just as assumed in the work of Dyson and Xuong after having noted the near mass degeneracy of the deuteron ground state D_{01} with the virtual 1S_0 state D_{10} . Obviously, the spin-isospin splitting for dibaryons is different from that of baryons [38].

Possibly this resonance was sensed already before in the pionic double charge exchange reaction on nuclei. There the so-called nonanalog transitions exhibit an unexpected resonance-like behavior in the region of the Δ resonance [36,55,56]. For its explanation the DINT mechanism [57–60] was introduced, which in essence can be imagined as representing a ΔN system with $I(J^P) = 2(1^+)$ in the intermediate state [59].

V. SUMMARY AND CONCLUSIONS

Total and differential cross sections of the $pp \rightarrow pp\pi^+\pi^-$ reaction have been measured exclusively and kinematically complete in the energy range $T_p = 1.08$ – 1.36 GeV ($\sqrt{s} = 2.35$ – 2.46 GeV) by use of the quasifree process $pd \rightarrow pp\pi^+\pi^- + n_{\text{spectator}}$. The results for the total cross section are in good agreement with previous bubble-chamber data. For the differential cross sections there are no data available from previous measurements in the considered energy range.

The original Valencia calculations describing Roper and $\Delta\Delta$ excitations by t -channel meson exchange account well for the total cross section, but fail badly for the differential distributions of the $pp \rightarrow pp\pi^+\pi^-$ reaction. These calculations also have been shown to fail in other two-pion production channels, both for total and differential cross sections.

The differential cross sections for the $pp \rightarrow pp\pi^+\pi^-$ reaction are somewhat better accounted for by the modified Valencia calculations, but still fail strikingly for the $M_{pp\pi^-}$, $M_{pp\pi^+}$, and $\Theta_{\pi^+}^{c.m.}$ distributions. These calculations, which were tuned to the $pp \rightarrow pp\pi^0\pi^0$ and $pp \rightarrow nn\pi^+\pi^+$ reactions, have been shown to provide a good description of the other two-pion channels both in total and in differential cross sections. However, these so far very successful calculations predict also a much too small total cross section for the $pp\pi^+\pi^-$ channel at energies above $T_p \approx 0.9$ GeV.

This failure can be cured, if there is an opening of a new reaction channel near $T_p \approx 0.9$ GeV, i.e., near the $\Delta N\pi$ threshold, which nearly exclusively feeds the $pp\pi^+\pi^-$ channel. Such a process is given by the associated production of the isotensor ΔN state D_{21} with specific signatures in invariant mass spectra and in the π^+ angular distribution. We have demonstrated that such a process provides a quantitative description of the data for the $pp \rightarrow pp\pi^+\pi^-$ reaction, both for the total cross section and for all differential distributions.

This D_{21} state has been predicted already in 1964 by Dyson and Xuong [35] and more recently by Gal and Garcilazo [37], who also calculated its decay width. It is remarkable that five out of the six dibaryon states predicted in 1964 by considering SU(6) symmetry breaking have now been verified with masses very close to the predicted ones. For the sixth state, D_{30} , only upper limits have been found so far [61], but this subject deserves certainly further, more detailed investigations.

ACKNOWLEDGMENTS

We acknowledge valuable discussions with A. Gal, Ch. Hanhart, V. Kukuljin, and G. J. Wagner on this issue. We are particularly indebted to L. Alvarez-Ruso for using his code. We are also grateful to the anonymous referee of the Letter

version of this topic, who suggested that we look also into subsystem distributions. This work has been supported by DFG (CL214/3-1 and 3-2) and STFC (ST/L00478X/1) as well as by the Polish National Science Centre through the Grants No. 2016/23/B/ST2/00784 and No. 2013/11/N/ST2/04152.

-
- [1] L. G. Dakhno *et al.*, *Yad. Fiz.* **37**, 907 (1983) [*Sov. J. Nucl. Phys.* **37**, 540 (1983)].
- [2] C. D. Brunt, M. J. Clayton, and B. A. Wetswood, *Phys. Rev.* **187**, 1856 (1969).
- [3] F. Shimizu *et al.*, *Nucl. Phys. A* **386**, 571 (1982).
- [4] V. V. Sarantsev *et al.*, *Phys. At. Nucl.* **70**, 1885 (2007).
- [5] A. M. Eisner *et al.*, *Phys. Rev.* **138**, B670 (1965).
- [6] E. Pickup, D. K. Robinson, and E. O. Salant, *Phys. Rev.* **125**, 2091 (1962).
- [7] T. Tsuboyama, F. Sai, N. Katayama, T. Kishida, and S. S. Yamamoto, *Phys. Rev. C* **62**, 034001 (2000).
- [8] W. Brodowski, R. Bilger, H. Calen, H. Clement, C. Ekstrom, K. Fransson, J. Greiff, S. Haggstrom, B. Hoistad, J. Johanson, A. Johansson, T. Johansson, K. Kilian, S. Kullander, A. Kupsc, P. Marciniwski, B. Morosov, W. Oelert, J. Patzold, R. J. M. Y. Ruber, M. Schepkin, W. Scobel, I. Seluzhenkov, J. Stepaniak, A. Sukhanov, A. Turowiecki, G. J. Wagner, Z. Wilhelmi, J. Zabierowski, and J. Zlomanczuk, *Phys. Rev. Lett.* **88**, 192301 (2002).
- [9] J. Johanson *et al.*, *Nucl. Phys. A* **712**, 75 (2002).
- [10] J. Pätzold, M. Bashkanov, R. Bilger, W. Brodowski, H. Calen, H. Clement, C. Ekstrom, K. Fransson, J. Greiff, S. Haggstrom, B. Hoistad, J. Johanson, A. Johansson, T. Johansson, K. Kilian, S. Kullander, A. Kupsc, P. Marciniwski, B. Morosov, W. Oelert, R. J. M. Y. Ruber, M. Schepkin, W. Scobel, J. Stepaniak, A. Sukhanov, A. Turowiecki, G. J. Wagner, Z. Wilhelmi, J. Zabierowski, and J. Zlomanczuk, *Phys. Rev. C* **67**, 052202(R) (2003).
- [11] T. Skorodko *et al.*, *Eur. Phys. J. A* **35**, 317 (2008).
- [12] T. Skorodko *et al.*, *Phys. Lett. B* **679**, 30 (2009).
- [13] (a) F. Kren *et al.*, *Phys. Lett. B* **684**, 110 (2010); (b) **702**, 312 (2011); (c) see update of (a) in [arXiv:0910.0995](https://arxiv.org/abs/0910.0995) [nucl-ex].
- [14] T. Skorodko *et al.*, *Phys. Lett. B* **695**, 115 (2011).
- [15] T. Skorodko *et al.*, *Eur. Phys. J. A* **47**, 108 (2011).
- [16] M. Bashkanov, C. Bargholtz, M. Berlowski, D. Bogoslawsky, H. Calen, H. Clement, L. Demiroers, E. Doroshkevich, D. Duniec, C. Ekstrom, K. Fransson, L. Geren, L. Gustafsson, B. Hoistad, G. Ivanov, M. Jacewicz, E. Jiganov, T. Johansson, O. Khakimova, S. Keleta, I. Koch, F. Kren, S. Kullander, A. Kupsc, K. Lindberg, P. Marciniwski, R. Meier, B. Morosov, C. Pauly, H. Pettersson, Y. Petukhov, A. Povtorejko, A. Pricking, R. J. M. Y. Ruber, K. Schonning, W. Scobel, B. Shwartz, T. Skorodko, V. Sopov, J. Stepaniak, P. E. Tegner, P. Thorngren-Engblom, V. Tikhomirov, A. Turowiecki, G. J. Wagner, M. Wolke, J. Zabierowski, I. Zartova, and J. Zlomanczuk, *Phys. Rev. Lett.* **102**, 052301 (2009).
- [17] P. Adlarson *et al.*, *Phys. Lett. B* **706**, 256 (2012).
- [18] S. Abd El-Samad *et al.*, *Eur. Phys. J. A* **42**, 159 (2009).
- [19] S. Abd El-Bary *et al.*, *Eur. Phys. J. A* **37**, 267 (2008).
- [20] P. Adlarson *et al.*, *Phys. Rev. Lett.* **106**, 242302 (2011).
- [21] P. Adlarson *et al.*, *Eur. Phys. J. A* **52**, 147 (2016).
- [22] P. Adlarson *et al.*, *Phys. Lett. B* **721**, 229 (2013).
- [23] P. Adlarson *et al.*, *Phys. Rev. C* **88**, 055208 (2013).
- [24] P. Adlarson *et al.*, *Phys. Lett. B* **743**, 325 (2015).
- [25] G. Agakishiev *et al.*, *Phys. Lett. B* **750**, 184 (2015).
- [26] A. P. Jerusalemov *et al.*, *Eur. Phys. J. A* **51**, 83 (2015).
- [27] H. Clement, M. Bashkanov, and T. Skorodko, *Phys. Scr.* **T166**, 014016 (2015).
- [28] P. Adlarson *et al.*, *Phys. Rev. Lett.* **112**, 202301 (2014).
- [29] P. Adlarson *et al.*, *Phys. Rev. C* **90**, 035204 (2014).
- [30] R. L. Workman, W. J. Briscoe, and I. I. Strakovsky, *Phys. Rev. C* **93**, 045201 (2016).
- [31] L. Alvarez-Ruso, E. Oset, and E. Hernandez, *Nucl. Phys. A* **633**, 519 (1998) and private communication.
- [32] X. Cao, B.-S. Zou, and H.-S. Xu, *Phys. Rev. C* **81**, 065201 (2010).
- [33] A. V. Anisovich *et al.*, *Eur. Phys. J. A* **48**, 15 (2012).
- [34] Particle Data Group, K. A. Olive *et al.*, *Chin. Phys. C* **38**, 090001 (2014).
- [35] F. J. Dyson and N.-H. Xuong, *Phys. Rev. Lett.* **13**, 815 (1964).
- [36] H. Clement, *Prog. Part. Nucl. Phys.* **93**, 195 (2017).
- [37] A. Gal and H. Garcilazo, *Nucl. Phys. A* **928**, 73 (2014).
- [38] H. Huang, J. Ping, X. Zhu, and F. Wang, *Phys. Rev. C* **98**, 034001 (2018).
- [39] P. Adlarson *et al.*, *Phys. Rev. Lett.* **121**, 052001 (2018).
- [40] Ch. Bargholtz *et al.*, *Nucl. Instrum. Methods A* **594**, 339 (2008).
- [41] H. H. Adam *et al.*, [arXiv:nucl-ex/0411038](https://arxiv.org/abs/nucl-ex/0411038).
- [42] R. Machleidt, *Phys. Rev. C* **63**, 024001 (2001).
- [43] P. Adlarson *et al.*, *Phys. Rev. C* **91**, 015201 (2015).
- [44] M. Bashkanov and H. Clement, *Eur. Phys. J. A* **50**, 107 (2014).
- [45] N. Hoshizaki, *Prog. Theor. Phys.* **89**, 251 (1993).
- [46] R. A. Arndt, J. S. Hyslop, and L. D. Roper, *Phys. Rev. D* **35**, 128 (1987).
- [47] M. Bashkanov, H. Clement, and T. Skorodko, *Nucl. Phys. A* **958**, 129 (2017).
- [48] J. Zlomanczuk *et al.*, *Phys. Lett. B* **436**, 251 (1998).
- [49] R. Bilger *et al.*, *Nucl. Phys. A* **693**, 633 (2001).
- [50] C. Wilkin, *Eur. Phys. J. A* **53**, 114 (2017).
- [51] S. Abd El-Samad *et al.*, *Eur. Phys. J. A* **30**, 443 (2006).
- [52] V. Komarov, D. Tsirkov, T. Azaryan, Z. Bagdasarian, S. Dymov, R. Gebel, B. Gou, A. Kacharava, A. Khoukaz, A. Kulikov, V. Kurbatov, B. Lorentz, G. Macharashvili, D. Mchedlishvili, S. Merzliakov, S. Mikiirtychians, H. Ohm, M. Papenbrock, F. Rathmann, V. Serdyuk, V. Shmakova, H. Stroher, S. Trusov, Y. Uzikov, and Y. Valdau, *Phys. Rev. C* **93**, 065206 (2016).
- [53] E. Byckling and K. Kajantie, *Particle Kinematics* (John Wiley & Sons, London, 1973).
- [54] T. Risser and M. D. Shuster, *Phys. Lett. B* **43**, 68 (1973).
- [55] H. Clement, *Prog. Part. Nucl. Phys.* **29**, 175 (1992).
- [56] M. B. Johnson and C. L. Morris, *Ann. Rev. Part. Sci.* **43**, 165 (1993).

- [57] Mikkel B. Johnson, E. R. Siciliano, H. Toki, and A. Wirzba, *Phys. Rev. Lett.* **52**, 593 (1984).
- [58] R. Gilman, H. T. Fortune, M. B. Johnson, E. R. Siciliano, H. Toki, and A. Wirzba, *Phys. Rev. C* **32**, 349 (1985).
- [59] Mikkel B. Johnson and L. S. Kisslinger, *Phys. Lett. B* **168**, 26 (1986).
- [60] A. Wirzba, H. Toki, E. R. Siciliano, M. B. Johnson, and R. Gilman, *Phys. Rev. C* **40**, 2745 (1989).
- [61] P. Adlarson *et al.*, *Phys. Lett. B* **762**, 455 (2016).